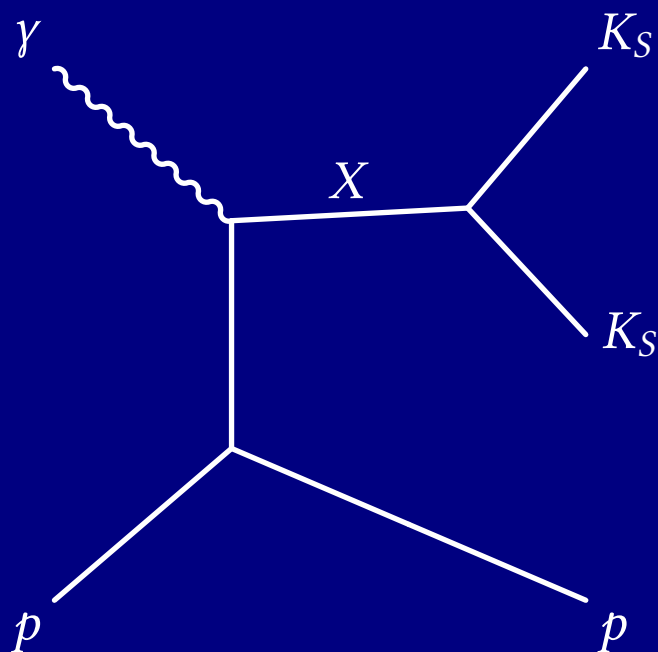# Introduction to $K_S K_S$ Physics at GlueX

Nathaniel Dene Hoffman

Carnegie Mellon University

Table of Contents

Chapter 1

Introduction

1.1   A Brief History of Particle Physics

Since the days of the ancient Greeks, scientists and philosophers alike have been interested in the fundamental question concerning the composition of the universe. While the Greeks maintained that the world was composed of four indivisible elemental substances (fire, earth, air, and water) [1], this was at best a guess by the early philosophers, who had no mechanism with which to test their theory. Ironically, these philosophers struggled with a question to which us modern physicists still have no answer: Are the building blocks of the natural world fundamental (indivisible) [2]?

In 1808, John Dalton published a manuscript which described what is now called the "law of multiple proportions" after compiling several observations on chemical reactions which occur with specific proportions of their reactants. He anglicized the Greek *atomos*, meaning "not able to be cut", into the word we are familiar with—"atom" [3]. Towards the end of the century, J. J. Thomson demonstrated that cathode rays could be deflected by an electrostatic field, an observation which could not be explained by the prevailing theory that the rays were some form of light [4]. Instead, he proposed that these rays were made up of charged particles he called "corpuscles" (later renamed to the familiar "electrons") [5]. Around the same time (between 1906 and 1913), Ernest Rutherford, Hans Geiger, and Ernest Marsden conducted experiments in which they scattered alpha particles through a thin metal foil, and, through an analysis of the scattering angles, concluded that a positively charged nucleus must exist at the center of atoms, surrounded by electrons [6].

Over the next several decades, the nucleus was further divided into protons and neutrons[1] [7, 8]. In 1964, Murray Gell-Mann and George Zweig proposed a theory that protons and neutrons (and all other baryons and mesons) were in fact composed of smaller particles Gell-Mann called "quarks"[2] [9]. These particles, along with the electron-like family of leptons (including neutrinos), the gauge bosons, and the Higgs boson, discovered in 2012 [10], comprise the Standard Model, a mathematical model which describes all the known forces and matter of the universe, with the notable exceptions (at time of writing) of gravity, dark matter, dark energy, and neutrino masses.

This thesis begins at a time when physicists are working hard to find gaps in this model, mostly by probing higher and higher ranges of energy. The experimental work being done at GlueX, however, resides in a lower regime, which we usually describe as "medium energy physics". As I will elucidate later in this manuscript, the strong force is non-perturbative in this regime, making direct calculations through the Standard Model all but impossible. However, since the advent of Lattice Quantum Chromodynamics (LQCD) in 1974 [11], physicists have been able to make approximate predictions via computer simulations of the theory.

---

[1]For the discovery of the electron and neutron, Thomson and James Chadwick won Nobel Prizes in Physics in 1906 and 1935, respectively. Rutherford won the 1908 Nobel Prize in Chemistry for his research in radiation. However, I want to emphasize that while I mention the "big names" here, there are many who contributed in relative obscurity.

[2]Upon reading the section of Finnegan's Wake which Gell-Mann cites as inspiration behind the name, I found (somewhat surprisingly) that the word "quark" was originally intended to rhyme with "mark", "ark", "lark", "bark", and so on, viz. [kwɑːrk] rather than the more common [kwɔːrk]!

1.2 Thesis Overview

Herein, I will focus on a particular portion of the Standard Model that dictates the strong interaction, viz. interactions between quarks and gluons, the mediating gauge boson of the strong force. I will also utilize some aspects of the weak force in my analysis concerning the decays of kaons. I will begin with a discussion of the theory and history of K_S (K-short) pair production in prior experiments, followed by a brief overview of the GlueX experiment. I will then outline some of the theoretical underpinnings and implications of glueballs to persuade the reader on the importance of this production channel in the larger scheme of GlueX.

Next, I will describe my own analysis, beginning with the the impetus of this study, a search for Σ^+ baryons using a different recombination of the final state in this channel. This will lead to a first-order peek at the many resonances which decay to K_S pairs, and I will delineate the layers of data selection which I carried out to produce a clean sample of events.

I will then discuss the process of partial-wave analysis (PWA), modeling resonances, and selecting a waveset for my data. I will conclude with the results from fits of these models to the data, the implications of such fits, and the next steps which I or another future particle physicist might take in order to illuminate another corner of the light mesonic spectrum.

1.3 Motivation

While this will be discussed in detail later, I believe it is important to emphasize the motivation for such a study of photoproduction of $K_S K_S$. While the majority of GlueX research concerns the study of hybrid mesons (mesons with forbidden quantum numbers), such mesons cannot be found in this channel. Given a bound state of two spin-$\frac{1}{2}$ quarks with relative angular momentum L, total spin S and total angular momentum J (the eigenvalue of $\hat{J}^2 = \hat{L}^2 \oplus \hat{S}^2$), we can define the parity operator $\hat{P}$ by its effect on the wave function of the system,

$$\hat{P} \left| \vec{r} \right\rangle = \eta \left| \vec{r} \right\rangle \tag{1.1}$$

where η can be determined by noting that states of angular momentum are generally proportional to a spherical harmonic in their angular distribution ($|r, \theta, \varphi; LM\rangle \sim Y_L^M(\theta, \varphi)$) and

$$\hat{P} Y_L^M(\theta, \varphi) = Y_L^M(\pi - \theta, \pi + \varphi) = (-1)^L Y_L^M(\theta, \varphi) \tag{1.2}$$

so $\eta = (-1)^L$. The Dirac equation can be used to show that the intrinsic parity of quarks and antiquarks, when multiplied, yields a factor of -1, so

$$\hat{P} \left| q\bar{q}; JLMS \right\rangle = -(-1)^L \tag{1.3}$$

Similarly, the operator $\hat{C}$ representing C-parity will also introduce a factor of $(-1)^L$ because exchanging charges of a (neutral[3]) quark-antiquark system is akin to reversing their positions under parity. If $|S\rangle$ is antisymmetric under C-parity, we should get an additional factor of -1, which is the case for the $S = 0$ singlet. With the aforementioned -1 due to the intrinsic parity of the quarks and antiquarks, we find

$$\hat{C}|q\bar{q}; JLMS\rangle = (-1)^{L+S} \tag{1.4}$$

Labeling states with the common J^{PC} notation, it can then be shown that states like $0^{--}, 0^{+-}, 1^{-+}$, and 2^{+-} (among others) are not allowed states for $q\bar{q}$ mesons. As mentioned, the investigation of such states is the primary focus of the GlueX experiment. However, since the particle we are concerned with decays to two identical particles (K_S) which have a symmetric spatial wave function, and because this particle is a meson which follows Bose-Einstein statistics, the angular part of the total wave function must also be symmetric, i.e. $J = $ even integers. Furthermore, because parity is conserved in strong decays, and the state of two identical particles is symmetric under parity, the decaying meson must also have $P = +$. Finally, the strong interaction also conserves C-parity, and both kaons are neutral, so we can determine the J^{PC} quantum numbers of the resonance to be even^{++}. There should be no overlap here with the aforementioned hybrid mesons, but that does not mean the channel is not of interest to GlueX and the larger scientific community. Particularly, the lowest lying glueball states are predicted to not only share these quantum numbers, but exist in the middle of the mass range produced by GlueX energies[12]. To add to this, the spin-0 isospin-0 light flavorless mesons, denoted as f_0-mesons, are supernumerary, either due to mixing with a supposed light scalar glueball or by the presence of a light tetraquark (or both)[13].

However, it would be an understatement to say that the $K_S K_S$ channel at GlueX is not the ideal place to be looking for either glueballs or tetraquarks. This is because, while we have excellent handles for reconstructing this channel, we have no ability to separate particles of different isospin with these data alone. This means that these f states will be indistinguishable from their isospin-1 partners, the a-mesons. At first glance, it might seem like a model of the masses of these particles would make it easy to separate them, even if they remained indistinguishable between resonant peaks, but with broad states like the $f_0(1370)$ and states which sit right on top of each other (like the $f_0(980)$ and $a_0(980)$, which also tend to interfere with each other), there is likely no unique mass model which can distinguish all of the possible states without relying on data from other channels.

The silver lining is that, due to the GlueX detector's state-of-the-art angular acceptance[14], we do stand a chance at separating spin-0 states from spin-2 states, and GlueX's polarized beam allows us to further understand the mechanisms at play by giving us some indication of the parity of the t-channel exchanged particle in the production interaction. We can also use this channel as a proving ground for more complex amplitude analysis involving a mass model, which could be extended to a coupled-channel analysis in the future.

---

[3]For $\hat{C}$ to be Hermitian, and thus observable, acting it twice on a state should return the original state, so only eigenvalues of ± 1 are allowed. Therefore, only states which are overall charge neutral are eigenstates of $\hat{C}$.

Chapter 2

Experimental Design and Data Selection

2.1   The GlueX Experiment

The GlueX Kinematic Fit

2.2   Data Selection for the $K_S K_S$ Channel

Fiducial Cuts

2.3   sPlot Weighting

At this stage in the analysis, we are running low on simple cuts which can improve the signal-to-background ratio in the dataset. We must now turn to more complex solutions of separating the signal from potential background seepage. The first method we will use to do this is sPlot[15][1], a weighting scheme which corrects the naïve probabilistic weights one might first think to construct (dubbed "inPlot").

We start by developing a model for the signal and background probability distribution functions (PDFs) for a "discriminating" variable. We could then weight each event by some normalized probability of it being in the signal distribution rather than the background:

$$w(x) = \frac{N_S f_S(x)}{N_S f_S(x) + N_B f_B(x)} \tag{2.1}$$

where x is the discriminating variable, $f_S(x)$ and $f_B(x)$ are the corresponding signal and background PDFs, and N_S and N_B are the total number of signal and background events, respectively.

However, as shown by Pivk and Le Diberder[15], we must be careful when using this procedure, as it will only correctly produce signal-isolated plots for "control" variables y which are directly correlated with x. For the time being, let us assume that this is not the case, and that we wish to use the distribution of some variable which is uncorrelated with the variables we are plotting and analyzing[2]. Following the sPlot derivation, we find that, to plot uncorrelated control variables, we must weight our data according to the following scheme:

$$w(x) = \frac{V_{SS} f_S(x) + V_{SB} f_B(x)}{N_S f_S(x) + N_B f_B(x)}, \quad \text{where } V_{ij}^{-1} = \sum_x \frac{f_i(x) f_j(x)}{(N_S f_S(x) + N_B f_B(x))^2} \tag{2.2}$$

The V^{-1} matrix can also be understood as the covariance matrix between the free parameters N_S and N_B in the fit of the signal-background mixture, $V_{ij}^{-1} = -N \frac{\partial^2 \ln \mathcal{L}}{\partial N_i \partial N_j}$, although there is reason to believe this will lead to less accurate results than the manual calculation in ??[16].

Now that we have a method of assigning weights, we must pick the discriminating variable. Typically, these weighting methods work well on the classic "bump-on-a-background" distributions, but because the mass of the kaons is constrained in the kinematic fit, the fitted mass of each kaon is just a δ-function and combination of measured masses for each $\pi^+ \pi^-$ pair will yield a Normal distribution with little to no apparent background (by construction). We must be a bit more clever in determining a discriminating variable! By examining the BGGEN analysis done in [TODO: PREVIOUS SECTION], we can see that most likely sources of background arise when the intermediate kaons are missing from the reaction: $\gamma p \to 4\pi p$. This reaction shares the $K_S K_S$ final state exactly, so pairs of pions which look close enough to kaons will be almost indistinguishable in the data. However, they differ in one key way, namely that the K_S intermediate contains a strange quark while the $\pi^+ \pi^-$ decay state does not, so such a decay must occur via the weak interaction, which is notably slower than the strong interaction which would produce pion

---

[1]This is stylized as $_s\mathcal{P}lot$ in the original paper, but I find this tedious to type and to read.
[2]We will later see that things are not quite so simple!

pairs with no intermediate kaon. In other words, while the signal's rest-frame lifetime distribution should have an exponential slope near the K_S lifetime, the background would theoretically have nearly zero rest-frame lifetime for every event, or a much smaller exponential slope in practice.

Therefore, we will begin by generating both a signal and background dataset in Monte Carlo. We then interpret both datasets as if they were our desired channel by running them through the GlueX reconstruction and reaction filter, as well as all of our selections up to this point. We can then fit the rest-frame lifetime of each dataset to an exponential model,

$$f(t) = \lambda \exp\{-\lambda t\} \tag{2.3}$$

where $\lambda \equiv 1/\tau$, the lifetime of the kaon in question. Since we have two independently decaying kaons, we should really form a joint distribution for both, where we will assume each kaon has the same average lifetime:

$$f(t_1, t_2) = \lambda^2 \exp\{-\lambda t_1\} \exp\{-\lambda t_2\} \tag{2.4}$$

Both the signal and background distributions can be modeled in this way, giving us only two free parameters, λ_S and λ_B for the signal and background respectively, to fit (see Figure 2.1 for an example of these fits).

Once we obtain nominal values for λ_S and λ_B from fits over the signal and background Monte Carlo, we can fix the exponential slopes to the fit values and perform a new fit to our real data with a mixture model (see Figure 2.2):

$$f(t_1, t_2) = z\lambda_S^2 \exp\{-\lambda_S t_1\} \exp\{-\lambda_S t_2\} + (1 - z)\lambda_B^2 \exp\{-\lambda_B t_1\} \exp\{-\lambda_B t_2\} \tag{2.5}$$

In the fit to data, only the fraction of signal to background, z, is floating. From its fit value, we can determine values of N_S and N_B to use in Equation (2.2) and complete the weighting procedure.
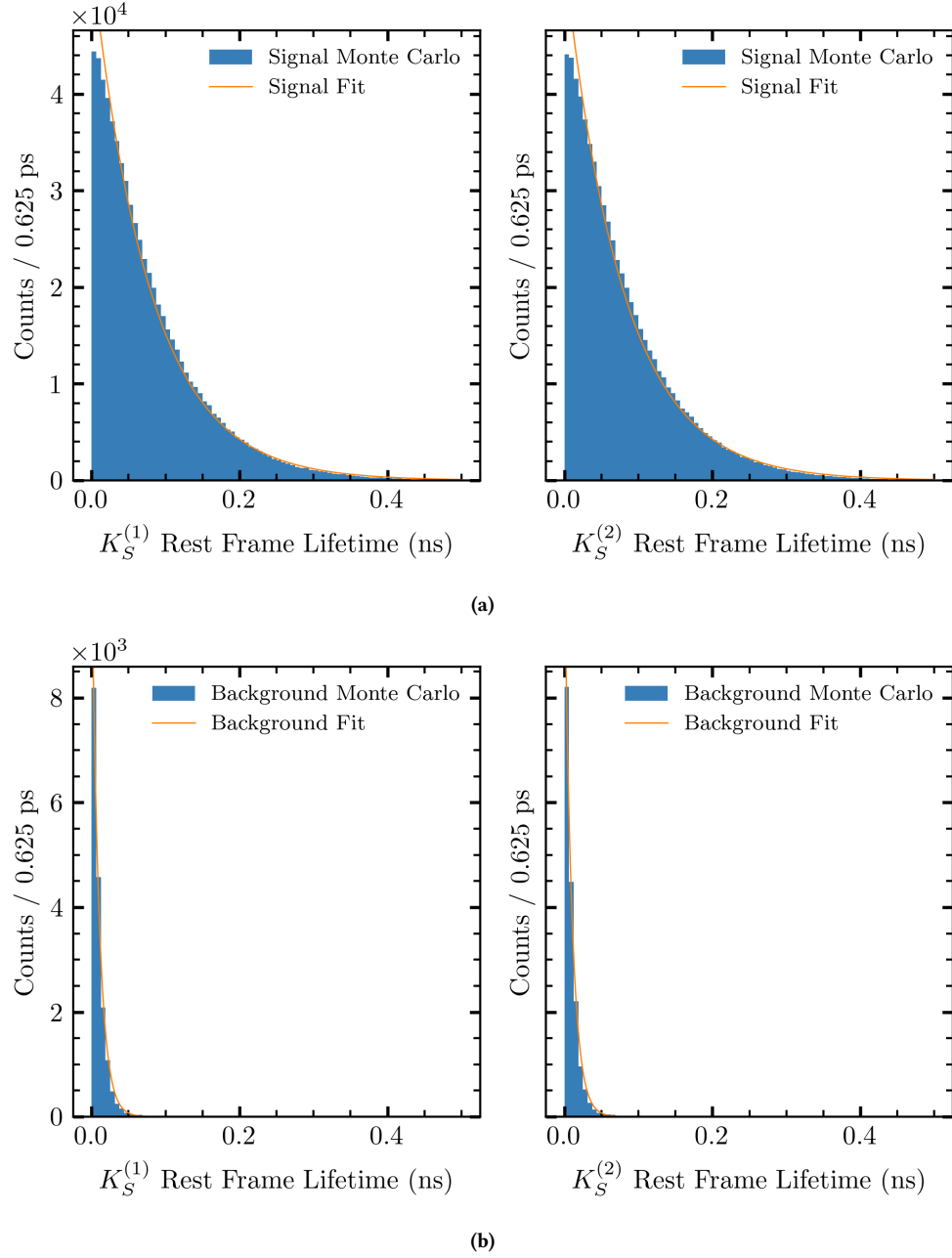
Figure 2.1: (a) Fit of an exponential product model to signal Monte Carlo generated using the F18 beam configuration. (b) The same fit as in (a), but over background Monte Carlo.TODO: zoom axis to 0.2 and plot signal MC as inset
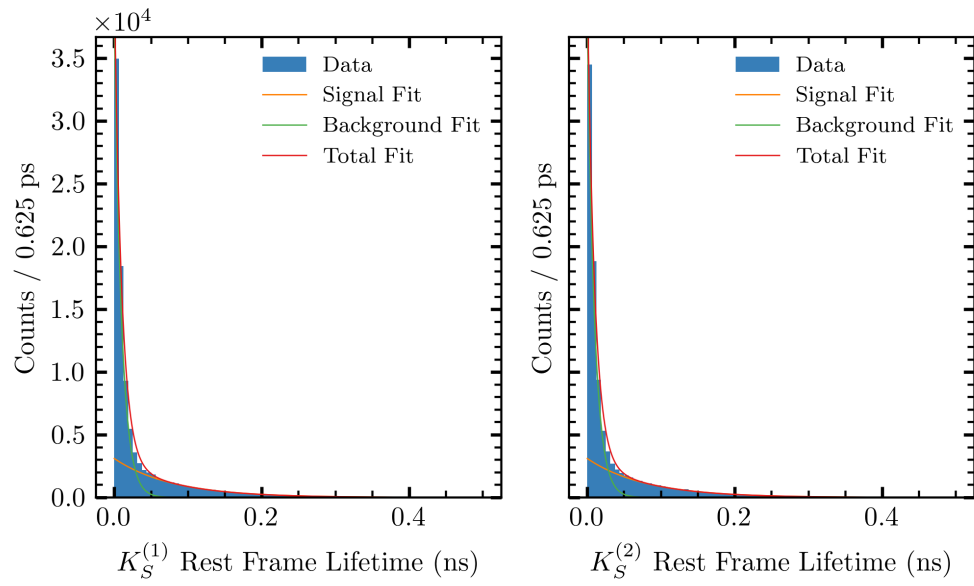
Figure 2.2: Fit of Equation (2.5) to data from the F18 run period. True kaon events are prominent in the tail of the distribution, which does not appear in background Monte Carlo samples (Figure 2.1b)TODO: zoom axis to 0.2

Chapter 3

Partial-Wave Analysis

3.1 Amplitude Formalism

formalisms We begin by representing a single particle with four-momentum $\mathbf{P} = (E, \vec{p})$, spin s, and helicity $\lambda = -s, -s+1, \ldots, s-1, s$ with the notation $\left|\vec{p}, s, \lambda\right\rangle$, a vector with Lorentz-invariant normalization

$$\left\langle \vec{p}', s', \lambda' \middle| \vec{p}, s, \lambda \right\rangle = (2\pi)^3 2E\delta^3(\vec{p}' - \vec{p})\delta_{s's}\delta\lambda'\lambda \tag{3.1}$$

Since we are primarily interested in two-body decays, we can then represent a two-body state using the notation

$$\left|\vec{p}_1, s_1, \lambda_1\right\rangle \otimes \left|\vec{p}_2, s_2, \lambda_2\right\rangle = \left|\vec{p}_1, s_1, \lambda_1; \vec{p}_2, s_2, \lambda_2\right\rangle \tag{3.2}$$

with normalization

$$\left\langle \vec{p}_1', s_1', \lambda_1'; \vec{p}_2', s_2', \lambda_2' \middle| \vec{p}_1, s_1, \lambda_1; \vec{p}_2, s_2, \lambda_2 \right\rangle = (2\pi)^6 4E_1 E_2 \delta^3(\vec{p}_1' - \vec{p}_1)\delta^3(\vec{p}_2' - \vec{p}_2)\delta_{s_1' s_1}\delta_{s_2' s_2}\delta_{\lambda_1' \lambda_1}\delta_{\lambda_2' \lambda_2} \tag{3.3}$$

For simplification, we will work in the center-of-momentum frame. This allows us to use a single momentum, $\vec{p}_1 = -\vec{p}_2$ without loss of generality in this frame. We can also assume that the spin of each particle is fixed and suppress s_1 and s_2 in the following derivations.

Next, we write the three-momentum in terms of spherical angles $\Omega_1 = (\theta_1, \varphi_1)$: $\vec{p}_1 = p_1(\sin\theta_1 \cos\varphi_1, \sin\theta_1 \sin\varphi_1, \cos\theta_1)$ where we use the shorthand $p_1 \equiv \left|\vec{p}_1\right|$. The equivalent coordinate transform must now be done on the normalization. It can be shown that,

$$\begin{aligned} \mathrm{d}^3\vec{p}_1\, \mathrm{d}^3\vec{p}_2 &= \mathrm{d}^3\vec{p}\, \mathrm{d}^3\vec{p}_1 \\ &= \mathrm{d}^3\vec{p}\, p_1^2\, \mathrm{d}(p_1)\, \mathrm{d}^2\Omega_1 \end{aligned} \tag{3.4}$$

where $\mathbf{P} = (E, \vec{p})$ is the total four-momentum in the center-of-momentum frame. Now note that, because we are in this frame, we can write $E = E_1 + E_2 = \sqrt{p_1^2 + m_1^2} + \sqrt{p_1^2 + m_2^2}$. Equivalently, we can write the differential element, $\mathrm{d}E$, as

$$\mathrm{d}E = p_1\, \mathrm{d}p_1 \left(\frac{1}{\sqrt{p_1 + m_1^2}} + \frac{1}{\sqrt{p_1 + m_2^2}} \right) = p_1\, \mathrm{d}p_1 \left(\frac{1}{E_1} + \frac{1}{E_2} \right) = \frac{\sqrt{s}}{E_1 E_2} p_1\, \mathrm{d}p_1 \tag{3.5}$$

where $s = E^2$ is the Mandelstam variable, so

$$\mathrm{d}^3\vec{p}_1\, \mathrm{d}^3\vec{p}_2 = \mathrm{d}^3\vec{p}\, \mathrm{d}E \frac{p_1 E_1 E_2}{\sqrt{s}} \mathrm{d}^2\Omega_1 = \frac{p_1 E_1 E_2}{\sqrt{s}} \mathrm{d}^4\mathbf{P}\mathrm{d}^2\Omega_1 \tag{3.6}$$

We can now take an arbitrary state and integrate over both sides:

$$\int \mathrm{d}^3\vec{p}_1\,\mathrm{d}^3\vec{p}_2\,\big\langle \vec{p}_1',\lambda_1';\vec{p}_2',\lambda_2'\big|\vec{p}_1,\lambda_1;\vec{p}2\lambda_2\big\rangle = \int \frac{p_1 E_1 E_2}{\sqrt{s}}\mathrm{d}^4\mathbf{P}\mathrm{d}^2\Omega_1\,\big\langle p_1',\Omega_1',\lambda_1',\lambda_2'\big|p_1,\Omega_1,\lambda_1,\lambda_2\big\rangle$$

$$(2\pi)^6 4E_1 E_2 \delta_{\lambda_1'\lambda_1}\delta_{\lambda_2'\lambda_2} = \int \frac{p_1 E_1 E_2}{\sqrt{s}}\mathrm{d}^4\mathbf{P}\mathrm{d}^2\Omega_1\,\big\langle p_1',\Omega_1',\lambda_1',\lambda_2'\big|p_1,\Omega_1,\lambda_1,\lambda_2\big\rangle$$

$$(2\pi)^6 \frac{4\sqrt{s}}{p_1}\delta_{\lambda_1'\lambda_1}\delta_{\lambda_2'\lambda_2} = \int \mathrm{d}^4\mathbf{P}\mathrm{d}^2\Omega_1\,\big\langle p_1',\Omega_1',\lambda_1',\lambda_2'\big|p_1,\Omega_1,\lambda_1,\lambda_2\big\rangle \tag{3.7}$$

$$\tag{3.8}$$

from Equation (3.3), so the normalization factor should then be

$$\big\langle p_1',\Omega_1',\lambda_1',\lambda_2'\big|p_1,\Omega_1,\lambda_1,\lambda_2\big\rangle = (2\pi)^6 \frac{4\sqrt{s}}{p_1}\delta^4(\mathbf{P}'-\mathbf{P})\delta^2(\Omega_1'-\Omega_1)\delta_{\lambda_1'\lambda_1}\delta_{\lambda_2'\lambda_2} \tag{3.9}$$

Since $\vec{p} = \vec{0}$ in the center-of-momentum frame, these states are eigenstates of the total four-momentum operator $\hat{\mathbf{P}}$, and we can factor it out as

$$|p_1,\Omega_1,\lambda_1,\lambda_2\rangle = (2\pi)^3 \sqrt{\frac{4\sqrt{s}}{p_1}}\,|\Omega_1,\lambda_1,\lambda_2\rangle\,|\mathbf{P}\rangle \tag{3.10}$$

We can then imagine replacing the two-body system with a single decaying particle. Such a particle can be defined in terms of its total angular momentum, J, and the eigenvalue of $\hat{J}_z$, M. Such a basis is an eigenstate of $\hat{J}^2$ and therefore transforms under rotations as

$$|p_1,J,M,\lambda_1,\lambda_2\rangle \xrightarrow{R(\alpha,\beta,\gamma)} \sum_{M'} D_{M'M}^J(\alpha,\beta,\gamma)|p_1,J,M',\lambda_1,\lambda_2\rangle \tag{3.11}$$

where $D_{M'M}^J(\alpha,\beta,\gamma)$ is the Wigner D-matrix with Euler angles α, β, and γ. Next, we can define the transformation between our two-particle state and the single-particle state:

$$|p_1,\Omega_1,\lambda_1,\lambda_2\rangle = \sum_{JM} c_{JM}(p_1,\Omega_1,\lambda_1,\lambda_2)|p_1,J,M,\lambda_1,\lambda_2\rangle$$

$$|p_1,(0,0),\lambda_1,\lambda_2\rangle = \sum_{J} c_{J\lambda}(p_1,(0,0),\lambda_1,\lambda_2)|p_1,J,\lambda,\lambda_1,\lambda_2\rangle \tag{3.12}$$

where $\lambda = \lambda_1 - \lambda_2$ is the eigenvalue of $\hat{J}_z$ for the state where $\theta_1 = \phi_1 = 0$, or $\vec{p}_1 = p_1\hat{z} = -\vec{p}_2$. To rotate from this specific choice back to an arbitrary Ω_1, we apply a rotation $R(\varphi_1,\theta_1,-\varphi_1)$ according to Equation (3.11):

$$|p_1,\Omega_1,\lambda_1,\lambda_2\rangle = \sum_{J\lambda} c_{J\lambda}(p_1,(0,0),\lambda_1,\lambda_2)\,D_{M'\lambda}^J(\varphi_1,\theta_1,-\varphi_1)|p_1,J,M',\lambda_1,\lambda_2\rangle \tag{3.13}$$

$$\sum_{JM} c_{JM}(p_1,\Omega_1,\lambda_1,\lambda_2)|p_1,J,M',\lambda_1,\lambda_2\rangle = \sum_{J\lambda} c_{J\lambda}(p_1,(0,0),\lambda_1,\lambda_2)\,D_{M'\lambda}^J(\varphi_1,\theta_1,-\varphi_1)|p_1,J,M',\lambda_1,\lambda_2\rangle \tag{3.14}$$

so

$$c_{JM}(p_1, \Omega_1, \lambda_1, \lambda_2) = c_{J\lambda}(p_1, (0,0), \lambda_1, \lambda_2) D^J_{M\lambda}(\varphi_1, \theta_1, -\varphi_1) \tag{3.15}$$

By the Schur orthogonality relations applied to the Wigner D-matrices, we find that, without loss of generality,

$$c_{JM} = c_J = \sqrt{\frac{2J+1}{4\pi}} \tag{3.16}$$

so that

$$|p_1, \Omega_1, \lambda_1, \lambda_2\rangle = \sum_{JM} \sqrt{\frac{2J+1}{4\pi}} D^J_{M\lambda}(\varphi_1, \theta_1, -\varphi_1) |p_1, J, M, \lambda_1, \lambda_2\rangle \tag{3.17}$$

or

$$|p_1, J, M, \lambda_1, \lambda_2\rangle = \sqrt{\frac{2J+1}{4\pi}} \int d\Omega_1 \, D^{J*}_{M\lambda}(\varphi_1, \theta_1, -\varphi_1) |p_1, \Omega_1, \lambda_1, \lambda_2\rangle \tag{3.18}$$

From this, it can also be shown that

$$\langle J, M, \lambda'_1, \lambda'_2 | \Omega_1, \lambda_1, \lambda_2\rangle = \delta_{\lambda'_1 \lambda_1} \delta_{\lambda'_2 \lambda_2} \sqrt{\frac{2J+1}{4\pi}} D^J_{M\lambda}(\varphi_1, \theta_1, -\varphi_1) \tag{3.19}$$

Finally, these states are also eigenstates of $\hat{\mathbf{P}}$ since we are still working in the frame where $\vec{p} = \vec{0}$:

$$|p_1, J, M, \lambda_1, \lambda_2\rangle = (2\pi)^3 \sqrt{\frac{4\sqrt{s}}{p_1}} |J, M, \lambda_1, \lambda_2\rangle |\mathbf{P}\rangle \tag{3.20}$$

Two-to-Two Scattering

Let us now apply this to a two-to-two scattering problem $a + b \rightarrow c + d$ (which we will later apply to $\gamma p \rightarrow Xp$). We can write the initial and final states, working in the center-of-momentum frame, according to Equation (3.10). We will choose an initial frame where $\vec{p}_a \equiv p_i \hat{z} = -\vec{p}_b$. By definition, the final state momentum can also be defined relative to either particle, so we can choose $\vec{p}_f \equiv \vec{p}_c = -\vec{p}_d$:

$$|i\rangle = (2\pi)^3 \sqrt{\frac{4\sqrt{s}}{p_i}} |(0,0), \lambda_a, \lambda_b\rangle |\mathbf{P_i}\rangle \tag{3.21}$$

$$|f\rangle = (2\pi)^3 \sqrt{\frac{4\sqrt{s}}{p_f}} |\Omega_f, \lambda_a, \lambda_b\rangle |\mathbf{P_f}\rangle \tag{3.22}$$

We can define a scattering amplitude between state $|i\rangle$ and $|j\rangle$ as S such that

$$\langle f|S|i\rangle = (2\pi)^6 \sqrt{\frac{16s}{p_i p_f}} \langle \mathbf{P}_f| \langle \Omega_f, \lambda_c, \lambda_d|S|(0,0), \lambda_a, \lambda_b \rangle |\mathbf{P}_i\rangle$$

$$= (2\pi)^6 \langle \mathbf{P}_f|\mathbf{P}_i\rangle \sqrt{\frac{16s}{p_i p_f}} \langle \Omega_f, \lambda_c, \lambda_d|S(s)|(0,0), \lambda_a, \lambda_b \rangle$$

$$= (2\pi)^6 \delta^4 \left(\mathbf{P}_f - \mathbf{P}_i\right) \sqrt{\frac{16s}{p_i p_f}} \langle \Omega_f, \lambda_c, \lambda_d|S(s)|(0,0), \lambda_a, \lambda_b \rangle \tag{3.23}$$

Since we mostly do not care about the case where the initial and final states are the same, we will define (by convention) a transition amplitude which factors out such scatterings:

$$S_{fi} = \delta_{fi} + \iota(2\pi)^4 \delta^4(\mathbf{P}_f - \mathbf{P}_i) T_{fi} \tag{3.24}$$

such that

$$\langle f|T|i\rangle = -\iota(2\pi)^2 \sqrt{\frac{16s}{p_f p_i}} \langle \Omega_f, \lambda_c, \lambda_d|T(s)|(0,0), \lambda_a, \lambda_b \rangle \tag{3.25}$$

By inserting a complete set of states for both the initial and final two-particle systems:

TODO: Fix box

$$\langle f|T|i\rangle = -\iota(2\pi)^2 \sqrt{\frac{16s}{p_f p_i}} \langle \Omega_f, \lambda_f, \lambda_d| \left(\sum_{JM} |J, M, \lambda_c, \lambda_d\rangle \langle J, M, \lambda_c, \lambda_d| \right) T(s) \left(\sum_{J'M'} |J', M', \lambda_a, \lambda_b\rangle \langle J', M', \lambda_a, \lambda_b| \right) |(0,0), \lambda_a, \lambda_b\rangle \tag{3.26}$$

From Equation (3.17), we can write this as

$$\langle f|T|i\rangle = -\iota(2\pi)^2 \sqrt{\frac{16s}{p_f p_i}} \sum_{JMJ'M'} \sqrt{\frac{2J+1}{4\pi}} \sqrt{\frac{2J'+1}{4\pi}} D^{J*}_{M\lambda_f}(\varphi_f, \theta_f, -\varphi_f) \langle J, M, \lambda_c, \lambda_d|T(s)|J', M', \lambda_a, \lambda_b \rangle D^{J'}_{M'\lambda_f}(0,0,0)$$

$$= -\iota(2\pi)^2 \sqrt{\frac{16s}{p_f p_i}} \sum_{JMJ'M'} \sqrt{\frac{2J+1}{4\pi}} \sqrt{\frac{2J'+1}{4\pi}} D^{J*}_{M\lambda_f}(\varphi_f, \theta_f, -\varphi_f)\delta_{JJ'}\delta_{MM'} \langle \lambda_c, \lambda_d|T^J(s)|\lambda_a, \lambda_b \rangle D^{J'}_{M'\lambda_f}(0,0,0)$$

$$= -\iota(2\pi)^2 \sqrt{\frac{16s}{p_f p_i}} \sum_{J} \left(\frac{2J+1}{4\pi}\right) D^{J*}_{\lambda_i\lambda_f}(\varphi_f, \theta_f, -\varphi_f) \langle \lambda_c, \lambda_d|T^J(s)|\lambda_a, \lambda_b \rangle \tag{3.27}$$

where $\lambda_i \equiv \lambda_a - \lambda_b$ and $\lambda_f \equiv \lambda_c - \lambda_d$. The Wigner D-matrix is related to Wigner's small d-matrix by

$$D^{j*}_{m'm}(\alpha, \beta, \gamma) \equiv e^{\iota m'\alpha} d^{j}_{m'm}(\beta) e^{\iota m\gamma} \tag{3.28}$$

so we can also write

$$\langle f|T|i\rangle = -\imath(2\pi)^2 \sqrt{\frac{16s}{p_f p_i}} \sum_J \left(\frac{2J+1}{4\pi}\right) e^{-\imath(\lambda_f - \lambda_i)\varphi_f} d^J_{\lambda_i \lambda_j}(\theta_f) \langle \lambda_c, \lambda_d | T^J(s) | \lambda_a, \lambda_b \rangle$$

$$= -\imath(2\pi)^2 \sqrt{\frac{16s}{p_f p_i}} \sum_J \left(\frac{2J+1}{4\pi}\right) e^{-\imath(\lambda_f - \lambda_i)\varphi_f} d^J_{\lambda_i \lambda_j}(\theta_f) T^J_{\lambda_c, \lambda_d; \lambda_a, \lambda_b}(s)$$

$$= (-\imath)4\pi \sqrt{\frac{s}{p_f p_i}} \sum_J (2J+1) e^{-\imath(\lambda_f - \lambda_i)\varphi_f} d^J_{\lambda_i \lambda_j}(\theta_f) T^J_{\lambda_c, \lambda_d; \lambda_a, \lambda_b}(s) \tag{3.29}$$

The actual observable we care about is the differential cross section,

$$\frac{\partial^2 \sigma}{\partial s \partial \Omega_f} \propto |\langle f|T|i\rangle|^2 \tag{3.30}$$

so we can ignore the overall factor of $-\imath$ in Equations (3.27) and (3.29).

Two-Body Decays

Next, we will give a similar treatment to a particle $d \to 1 + 2$ where X is a particle with mass m_X, spin J_X, and spin projection M_X. Again, we will work in the center-of-momentum frame of this decay, so we can chose $\vec{p}_f \equiv \vec{p}_1 = -\vec{p}_2$. In the rest frame of particle X, we get the relation $s_X \equiv E_X^2 = m_X^2$ From Equation (3.10), we write the final state as

$$|f\rangle = (2\pi)^3 \sqrt{\frac{4m_X}{p_f}} |\Omega_f, \lambda_1, \lambda_2\rangle |\mathbf{P}_f\rangle \tag{3.31}$$

while the initial state has no dependence on the final state helicities and is given by

$$|i\rangle = |J, M\rangle |\mathbf{P}_X\rangle \tag{3.32}$$

Given a decay amplitude A which functions like our scattering matrix S in Equation (3.23), we can write

$$\langle f|A|i\rangle = (2\pi)^3 \sqrt{\frac{4m_X}{p_f}} \langle \Omega_f, \lambda_1, \lambda_2 | A | J_X, M_X \rangle$$

$$= (2\pi)^3 \sqrt{\frac{4m_X}{p_f}} \langle \Omega_f, \lambda_1, \lambda_2 | \left(\sum_{J'M'} |J', M', \lambda_1, \lambda_2\rangle \langle J', M', \lambda_1, \lambda_2| \right) A | J_X, M_X \rangle$$

$$= (2\pi)^3 \sqrt{\frac{4m_X}{p_f}} \sum_{J'M'} \sqrt{\frac{2J'+1}{4\pi}} D^{J'*}_{M'\lambda}(\varphi_f, \theta_f, -\varphi_f) \langle J', M', \lambda_1, \lambda_2 | A | J_X, M_X \rangle \tag{3.33}$$

where the last line comes from Equation (3.19). Since $\langle J', M' | J_X, M_X \rangle = \delta_{J'J_X} \delta_{M'M_X}$, (see Equation (3.18)), and because the matrix element should be rotationally invariant, we can write $\langle J', M', \lambda_1, \lambda_2 | A | J_X, M_X \rangle \equiv \delta_{J'J_X} \delta_{M'M_X} A_{\lambda_1 \lambda_2}$:

$$\langle f|A|i\rangle = (2\pi)^3 \sqrt{\frac{4m_X}{p_f}} \sqrt{\frac{2J_X+1}{4\pi}} D^{J_X*}_{M_X\lambda}(\varphi_f, \theta_f, -\varphi_f) A_{\lambda_1 \lambda_2} \tag{3.34}$$

Again, to relate this to an actual experimental observable, we take the square of the norm. Because we don't actually measure the helicities λ_1 or λ_2 in the GlueX experiment, we can instead sum over them:

$$\frac{\partial \sigma}{\partial \Omega_f} = \sum_{\lambda_1 \lambda_2} (2\pi)^3 \frac{2J_X + 1}{\pi} \frac{m_X}{p_f} \left| D^{J_X *}_{M_X \lambda}(\varphi_f, \theta_f, -\varphi_f) A_{\lambda_1 \lambda_2} \right|^2 \tag{3.35}$$

Production Amplitudes

TODO: cite https://link.springer.com/article/10.1140/epjc/s10052-020-7930-x Now we are ready to put everything together to work out a cross section for the reaction $\gamma + p \rightarrow [X \rightarrow K_S + K_S] + p'$. This is somewhat equivalent to combining Equation (3.27) and Equation (3.34), but the decay amplitude now includes the state of the spectator (recoil) proton. To temporarily maintain similar notation, we can write this reaction as $a + b \rightarrow c + X$ where $X \rightarrow 1 + 2$. We can write the matrix element as

3.2 Second attempt

Following https://onlinelibrary.wiley.com/doi/10.1155/2020/6674595

Including Linear Polarization

3.3 The Z^m_ℓ Amplitude

3.4 The K-Matrix Parameterization

3.5 Waveset Selection

Chapter 4

Results and Systematic Studies

4.1 Mass-Independent Fits

4.2 Mass-Dependent Fits

4.3 Systematics

Chapter 5

Conclusion

Appendix A

Derivation of the Chew-Mandelstam Function

We begin with the dispersion integral[1]:

$$C(s) = C(s_{\text{thr}}) - \frac{s - s_{\text{thr}}}{\pi} \int_{s_{\text{thr}}}^{\infty} ds' \, \frac{\rho(s')}{(s' - s)(s' - s_{\text{thr}})} \tag{A.1}$$

where $s_{\text{thr}} = (m_1 + m_2)^2$ and

$$\rho(s) = \sqrt{\left(1 - \frac{(m_1 + m_2)^2}{s}\right)\left(1 - \frac{(m_1 - m_2)^2}{s}\right)} \tag{A.2}$$

We first focus on just the integral part:

$$I(s) = \int_{s_{\text{thr}}}^{\infty} ds' \, \frac{\rho(s')}{(s' - s)(s' - s_{\text{thr}})} \tag{A.3}$$

$$\lim_{\epsilon \to 0} \int_{a}^{b} dx \, \frac{f(x)}{(x - x_0) + \iota\epsilon} = \fint_{a}^{b} dx \, \frac{f(x)}{(x - x_0)} + \iota\pi f(x_0) \tag{A.4}$$

$$I(s) = \fint_{s_{\text{thr}}}^{\infty} \tag{A.5}$$

---

[1] see arXiv paper

Bibliography

[1] Aristotle. *Metaphysics*. Trans. by W. D. Ross. 1.4,985b10-15. type: classic. URL: http://classics.mit.edu/Aristotle/metaphysics.html.

[2] Aristotle. *Physics*. Trans. by R. P. Hardie and R. K. Gaye. 6.1-3,231a21-234b10. URL: http://classics.mit.edu/Aristotle/physics.html.

[3] John Dalton. *A New System of Chemical Philosophy*. In collab. with Smithsonian Libraries. Manchester: Printed by S. Russell for R. Bickerstaff, Strand, London, 1808. 248 pp. URL: http://archive.org/details/newsystemofchemi11dalt (visited on 06/12/2024).

[4] J. J. Thomson. "Cathode Rays". In: *Philosophical Magazine* 44 (1897), pp. 293–316.

[5] J. J. Thomson. *The Corpuscular Theory of Matter*. Scribner's Sons, New York, 1907.

[6] E. Rutherford. "LXXIX. The scattering of α and β particles by matter and the structure of the atom". In: *The London, Edinburgh, and Dublin Philosophical Magazine and Journal of Science* 21.125 (May 1, 1911). Publisher: Taylor & Francis _eprint: https://doi.org/10.1080/14786440508637080, pp. 669–688. ISSN: 1941-5982. DOI: 10.1080/14786440508637080. URL: https://doi.org/10.1080/14786440508637080 (visited on 06/12/2024).

[7] Orme Masson. "XXIV. The constitution of atoms". In: *The London, Edinburgh, and Dublin Philosophical Magazine and Journal of Science* 41.242 (Feb. 1, 1921). Publisher: Taylor & Francis _eprint: https://doi.org/10.1080/14786442108636219, pp. 281–285. ISSN: 1941-5982. DOI: 10.1080/14786442108636219. URL: https://doi.org/10.1080/14786442108636219 (visited on 06/12/2024).

[8] J. Chadwick. "Possible Existence of a Neutron". In: *Nature* 129.3252 (Feb. 1932). Publisher: Nature Publishing Group, pp. 312–312. ISSN: 1476-4687. DOI: 10.1038/129312a0. URL: https://www.nature.com/articles/129312a0 (visited on 06/12/2024).

[9] M. Gell-Mann. "A schematic model of baryons and mesons". In: *Physics Letters* 8.3 (Feb. 1, 1964), pp. 214–215. ISSN: 0031-9163. DOI: 10.1016/S0031-9163(64)92001-3. URL: https://www.sciencedirect.com/science/article/pii/S0031916364920013 (visited on 06/12/2024).

[10]   G. Aad et al. "Observation of a new particle in the search for the Standard Model Higgs boson with the AT-
       LAS detector at the LHC". In: *Physics Letters B* 716.1 (Sept. 17, 2012), pp. 1–29. ISSN: 0370-2693. DOI: `10.`
       `1016/j.physletb.2012.08.020`. URL: `https://www.sciencedirect.com/science/`
       `article/pii/S037026931200857X` (visited on 06/12/2024).

[11]   Kenneth G. Wilson. "Confinement of quarks". In: *Physical Review D* 10.8 (Oct. 15, 1974). Publisher: American
       Physical Society, pp. 2445–2459. DOI: `10.1103/PhysRevD.10.2445`. URL: `https://link.aps.`
       `org/doi/10.1103/PhysRevD.10.2445` (visited on 06/12/2024).

[12]   Colin J. Morningstar and Mike Peardon. "Glueball spectrum from an anisotropic lattice study". In: *Physical
       Review D* 60.3 (July 7, 1999), p. 034509. ISSN: 0556-2821, 1089-4918. DOI: `10.1103/PhysRevD.60.`
       `034509`. URL: `https://link.aps.org/doi/10.1103/PhysRevD.60.034509` (visited on
       08/30/2024).

[13]   Particle Data Group et al. "Review of Particle Physics". In: *Progress of Theoretical and Experimental Physics*
       2020.8 (Aug. 14, 2020), p. 083C01. ISSN: 2050-3911. DOI: `10.1093/ptep/ptaa104`. URL: `https://`
       `academic.oup.com/ptep/article/doi/10.1093/ptep/ptaa104/5891211` (visited on
       08/30/2024).

[14]   S. Adhikari et al. "The GlueX beamline and detector". In: *Nuclear Instruments and Methods in Physics Re-
       search Section A: Accelerators, Spectrometers, Detectors and Associated Equipment* 987 (Jan. 2021), p. 164807. ISSN:
       01689002. DOI: `10.1016/j.nima.2020.164807`. URL: `https://linkinghub.elsevier.`
       `com/retrieve/pii/S0168900220312043` (visited on 08/30/2024).

[15]   M. Pivk and F.R. Le Diberder. "sPlot: A statistical tool to unfold data distributions". In: *Nuclear Instruments and
       Methods in Physics Research Section A: Accelerators, Spectrometers, Detectors and Associated Equipment* 555.1
       (Dec. 2005), pp. 356–369. ISSN: 01689002. DOI: `10.1016/j.nima.2005.08.106`. URL: `https://`
       `linkinghub.elsevier.com/retrieve/pii/S0168900205018024` (visited on 08/30/2024).

[16]   Hans Dembinski et al. "Custom Orthogonal Weight functions (COWs) for event classification". In: *Nuclear
       Instruments and Methods in Physics Research Section A: Accelerators, Spectrometers, Detectors and Associated
       Equipment* 1040 (Oct. 2022), p. 167270. ISSN: 01689002. DOI: `10.1016/j.nima.2022.167270`. URL:
       `https://linkinghub.elsevier.com/retrieve/pii/S0168900222006076` (visited on
       08/30/2024).